coatings

Supplementary Materials: Immobilized Nano-TiO_2 Photocatalysts for the Degradation of Three Organic Dyes in Single and Multi-Dye Solutions

Umberto Bellè [1], Filippo Pelizzari [1], Andrea Lucotti [2], Chiara Castiglioni [2], Marco Ormellese [1], MariaPia Pedeferri [1] and Maria Vittoria Diamanti [1,*]

[1] Department of Chemistry, Materials and Chemical Engineering "G. Natta", Politecnico di Milano, Via Mancinelli 7, Milan 20131, Italy; umberto.belle@polimi.it (U.B.); filippo.pelizzari@mail.polimi.it (F.P.); marco.ormellese@polimi.it (M.O.); mariapia.pedeferri@polimi.it (M.P.)
[2] Department of Chemistry, Materials and Chemical Engineering "G. Natta" Politecnico di Milano, Piazza Leonardo da Vinci 32, Milan 20133, Italy; andrea.lucotti@polimi.it (A.L.); chiara.castiglioni@polimi.it (C.C.)
* Correspondence: mariavittoria.diamanti@polimi.it; Tel.: +39-02-2399-3137

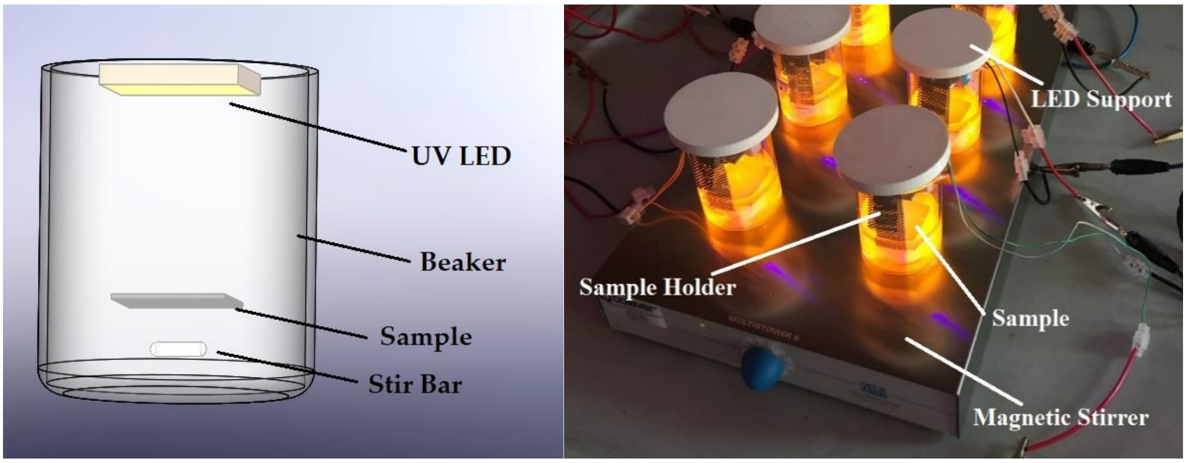

(**a**) (**b**)

Figure S1. (**a**) Schematic representation of the batch reactor used in this study (the TiO_2 nanotubular array is photoactivated by the LED positioned on top, at 3 cm from it). (**b**) Photograph of the batch reactor used in this study (it is possible to distinguish the beaker containing the solutions, the sample, the sample holder on which the sample is positioned, the magnetic stirrer and the 3D printed component that covers the beaker and supports the UV LED).

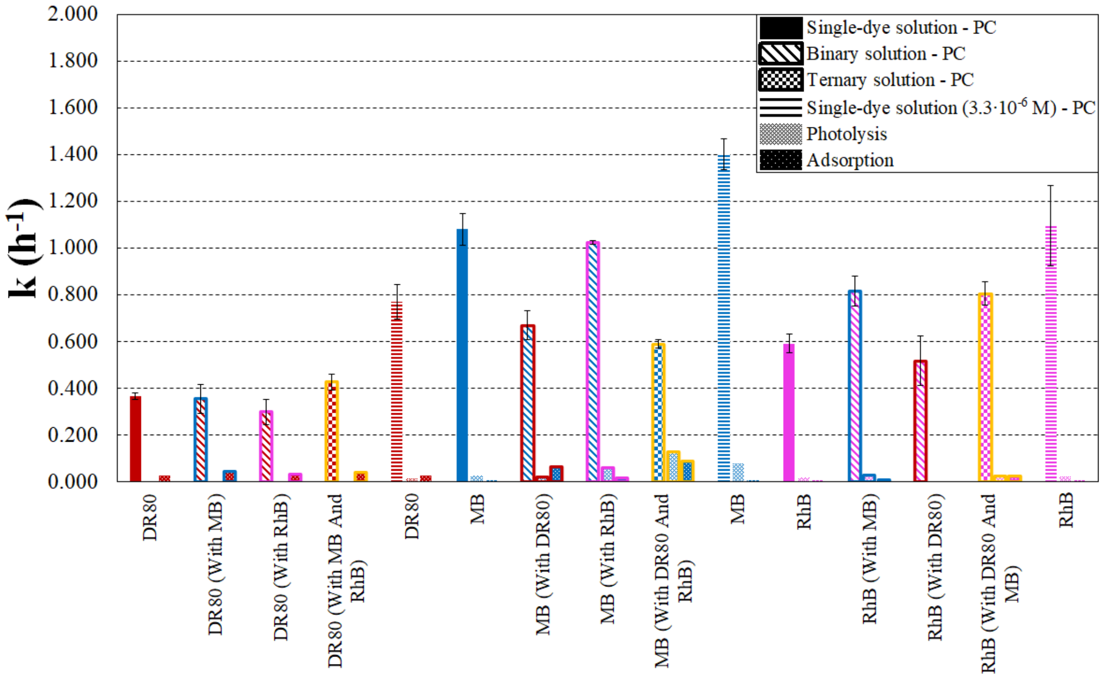

Figure S2. Kinetics of photocatalysis, photolysis and adsorption in the evaluated conditions ("PC" stands for photocatalysis).

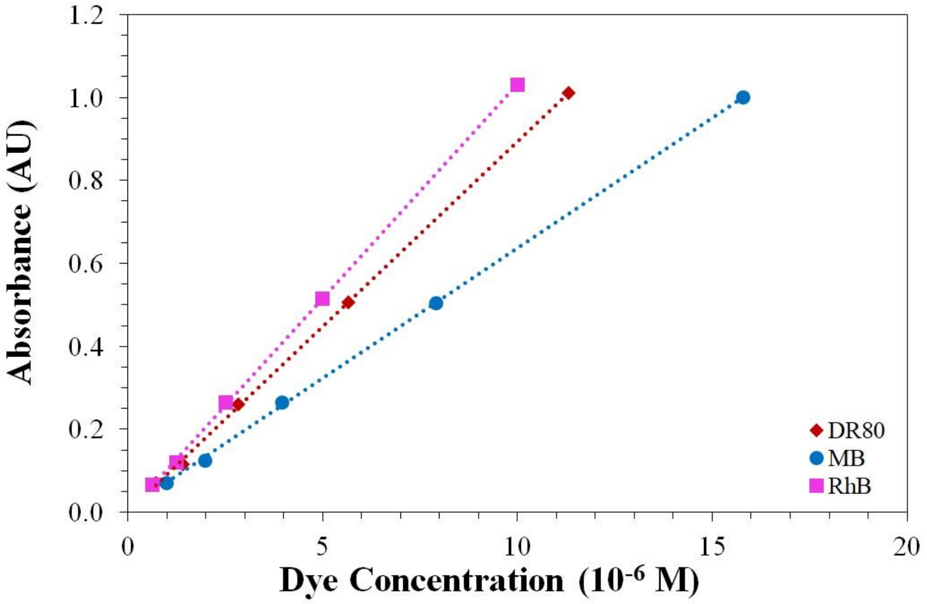

Figure S3. Calibration curves for dyes in single-dye solutions.

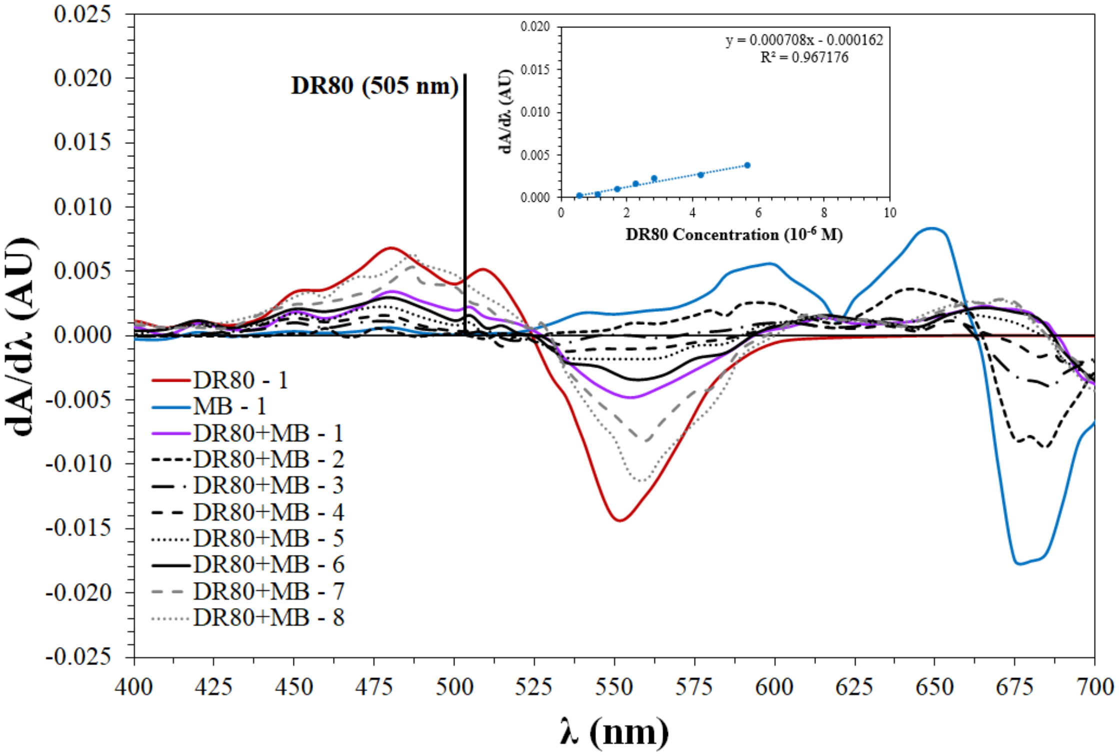

Figure S4. First-order derivative spectra of DR80, MB and DR80 + MB, at different DR80 concentrations, together with DR80 calibration curve. Dye concentrations of the solutions presented in this Figure are reported in Table S1 and in Table S2.

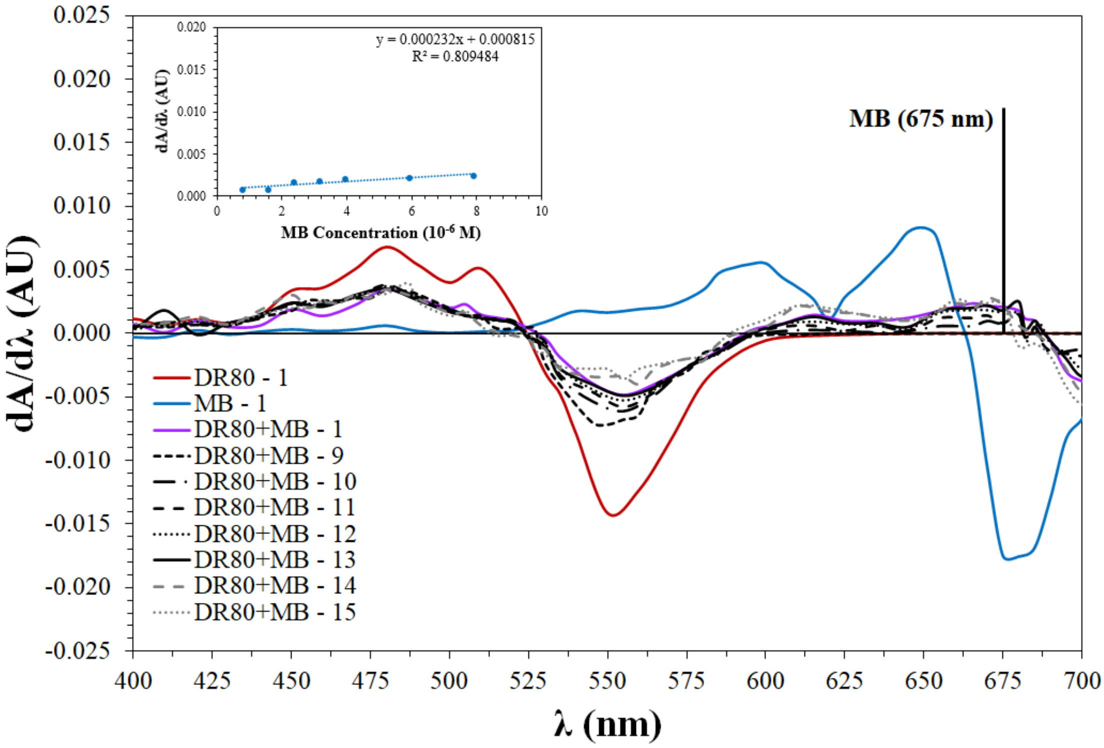

Figure S5. First-order derivative spectra of DR80, MB and DR80 + MB, at different MB concentrations, together with MB calibration curve. Dye concentrations of the solutions presented in this Figure are reported in Table S1 and in Table S2.

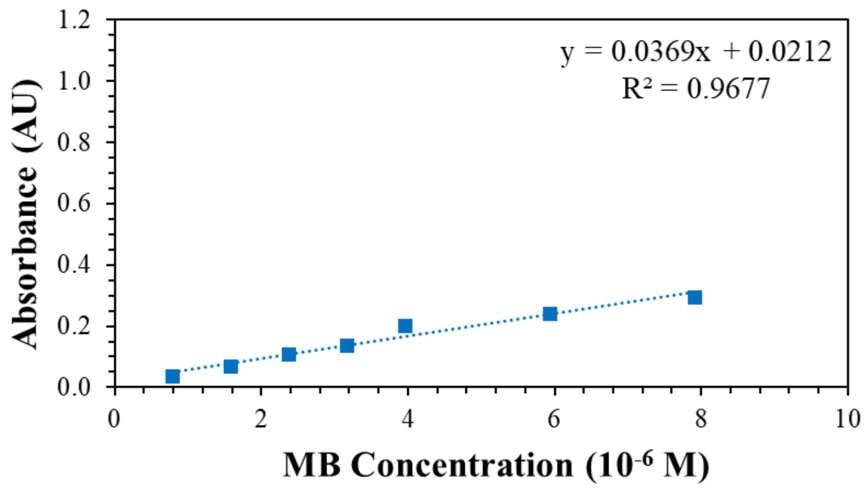

Figure S6. MB calibration curve in DR80 + MB system, evaluated at MB maximum absorbance peak (690 nm).

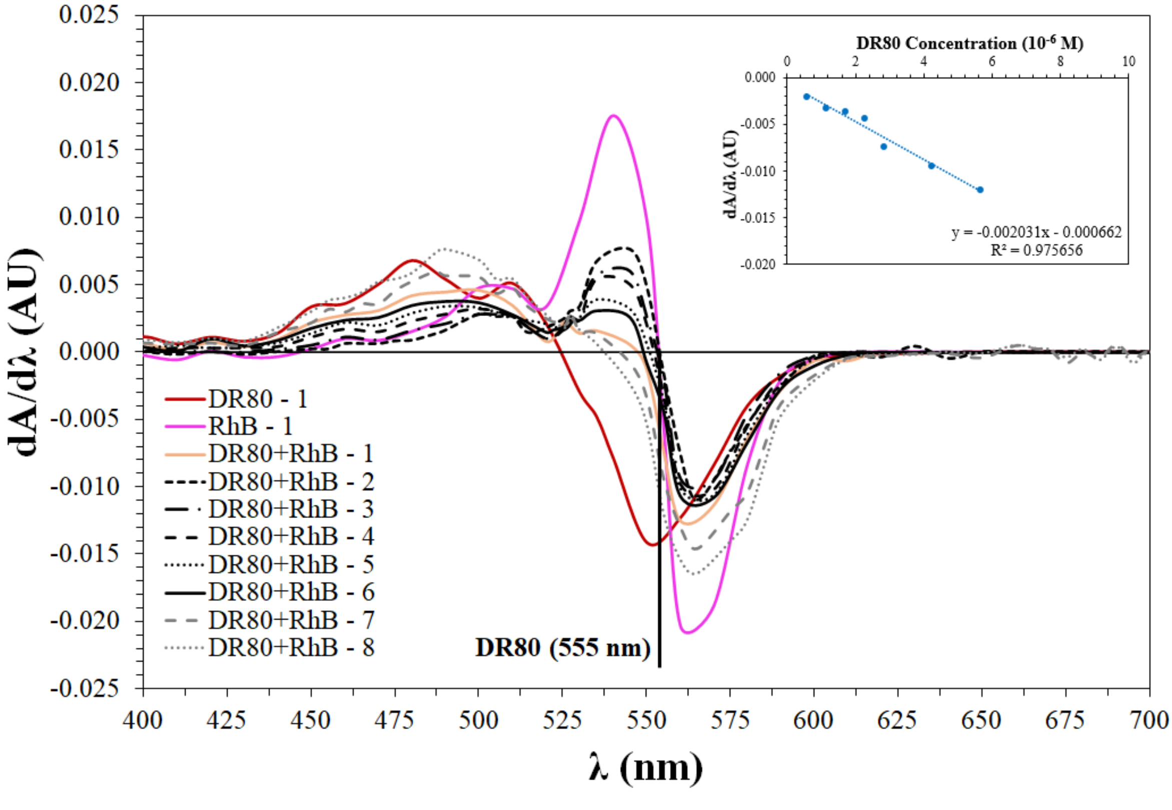

Figure S7. First-order derivative spectra of DR80, RhB and DR80 + RhB, at different DR80 concentrations, together with DR80 calibration curve. Dye concentrations of the solutions presented in this Figure are reported in Table S1 and in Table S2.

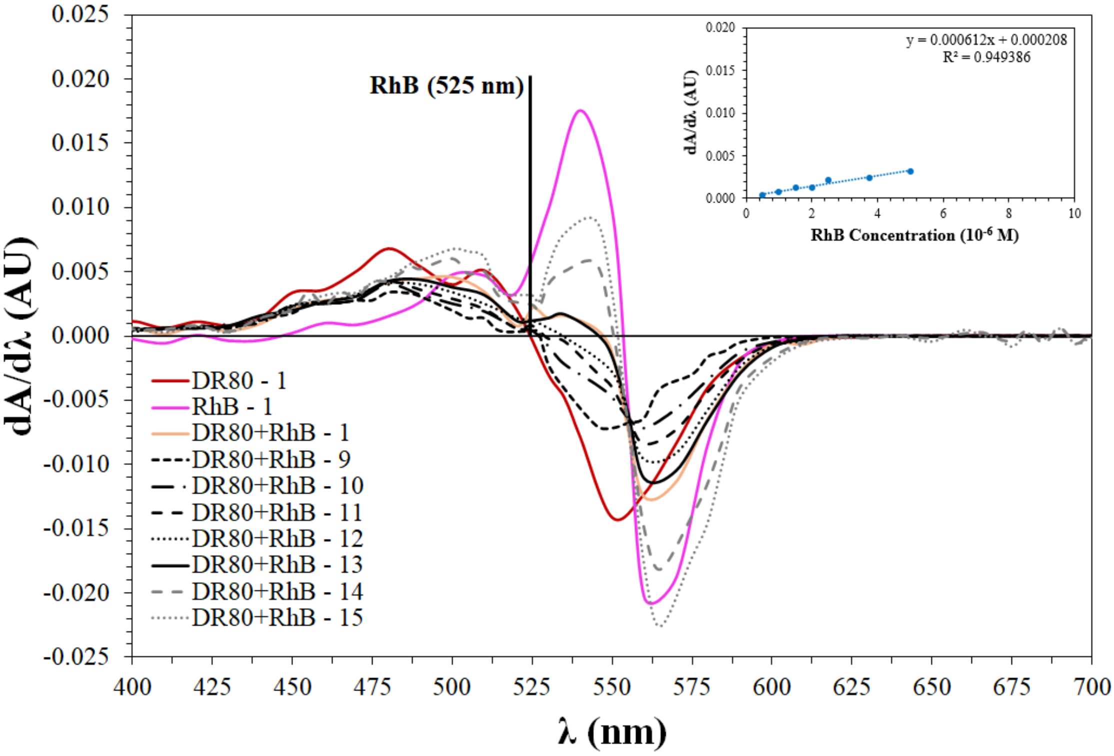

Figure S8. First-order derivative spectra of DR80, RhB and DR80 + RhB, at different RhB concentrations, together with RhB calibration curve. Dye concentrations of the solutions presented in this Figure are reported in Table S1 and in Table S2.

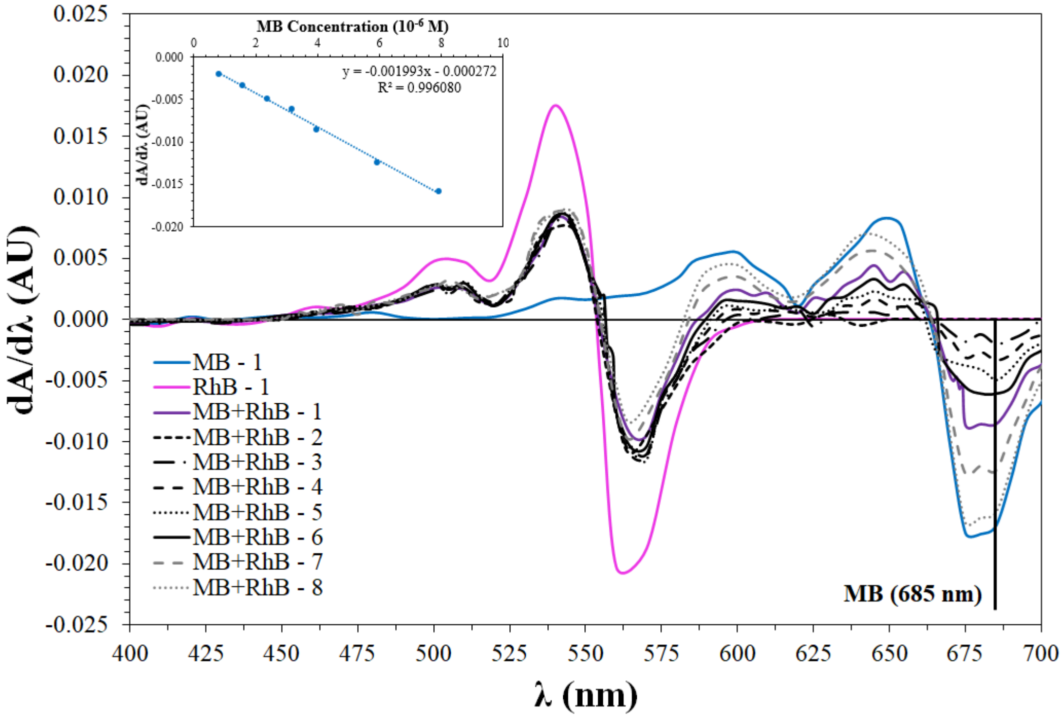

Figure S9. First-order derivative spectra of MB, RhB and MB + RhB, at different MB concentrations, together with MB calibration curve. Dye concentrations of the solutions presented in this Figure are reported in Table S1 and in Table S2.

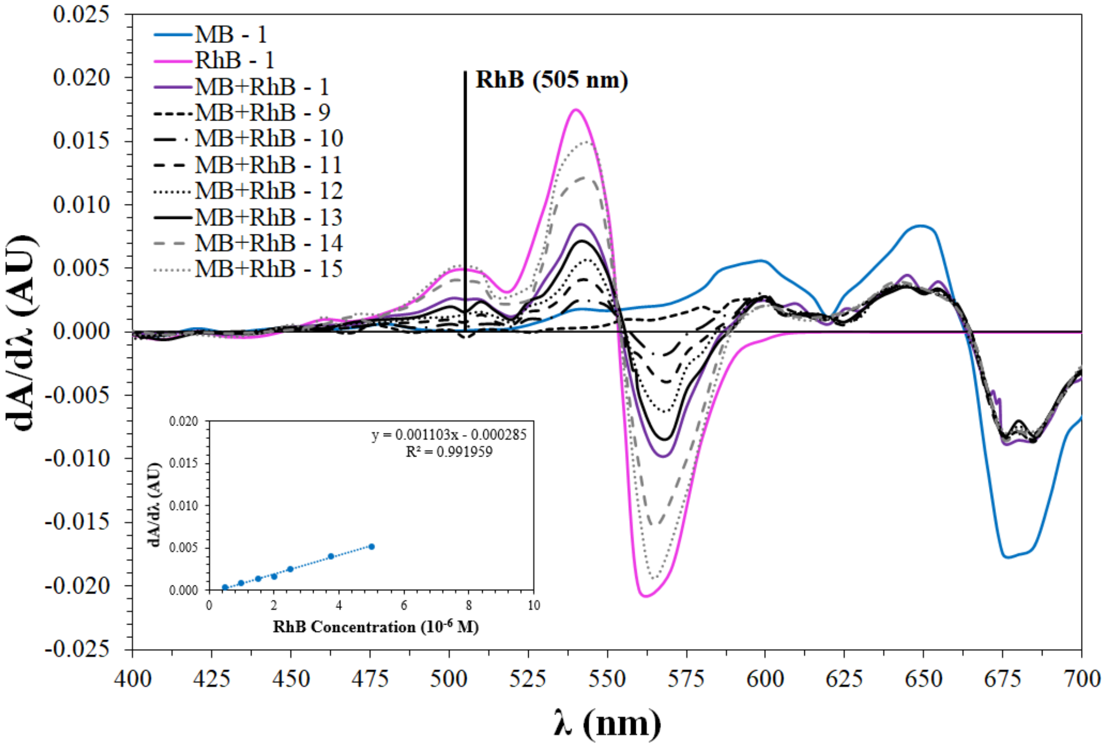

Figure S10. First-order derivative spectra of MB, RhB and MB + RhB, at different RhB concentrations, together with RhB calibration curve. Dye concentrations of the solutions presented in this Figure are reported in Table S1 and in Table S2.

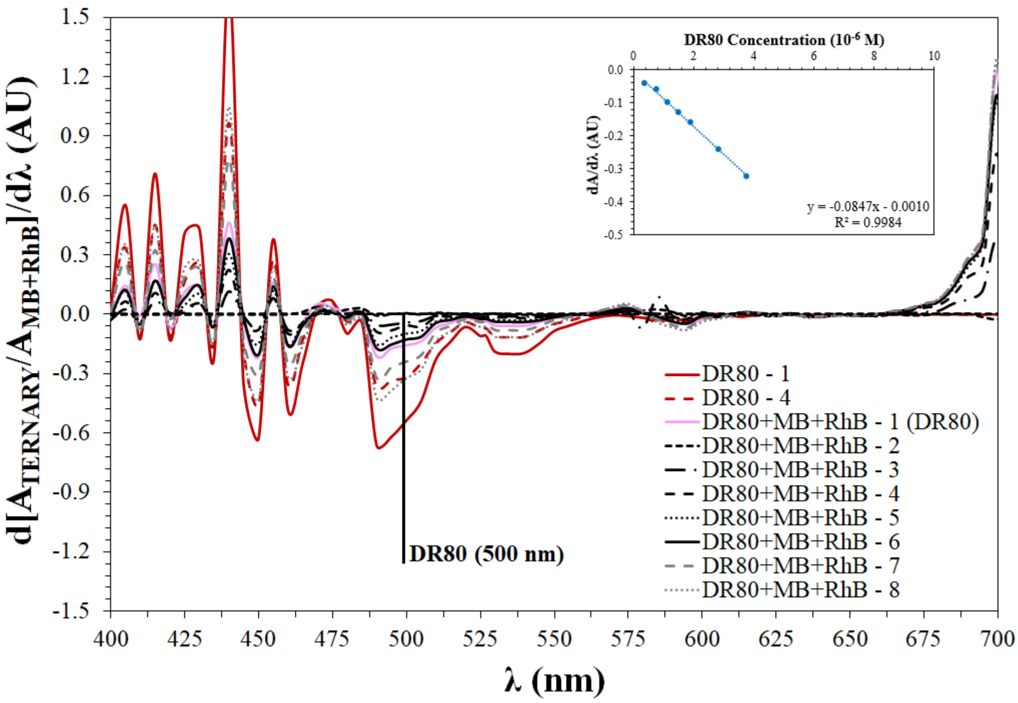

Figure S11. First-order derivative spectra of DR80 and DR80 + MB + RhB, at different DR80 concentrations, together with DR80 calibration curve. Dye concentrations of the solutions presented in this Figure are reported in Table S1 and in Table S3.

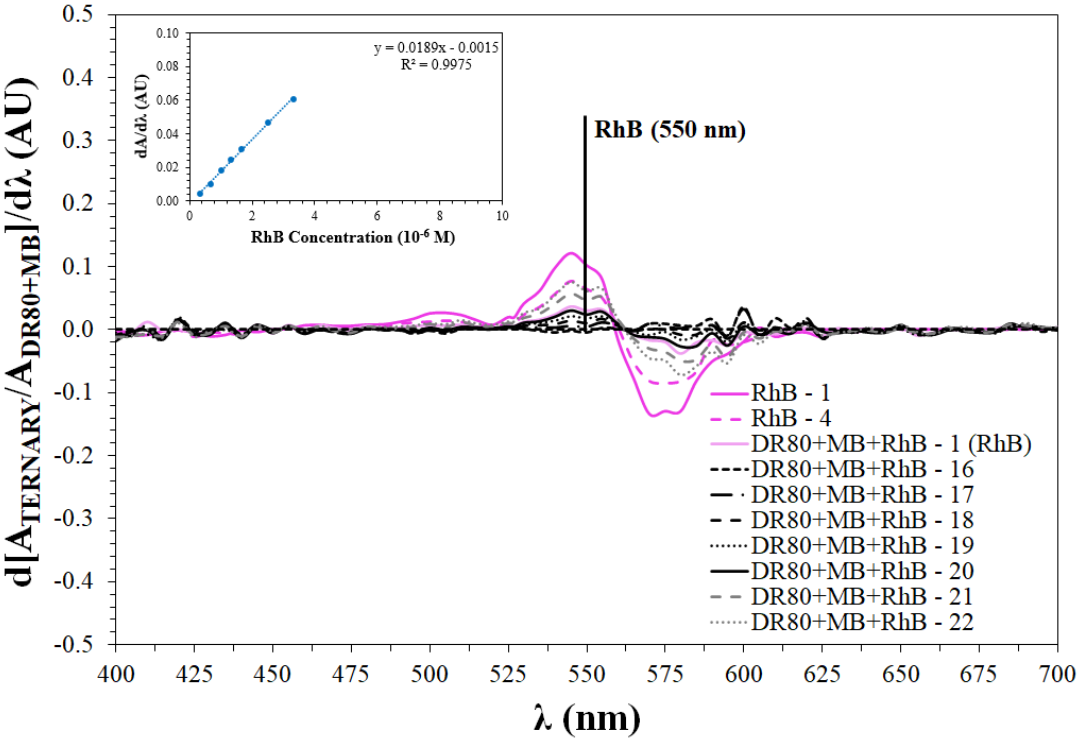

Figure S12. First-order derivative spectra of DR80 and DR80 + MB + RhB, at different RhB concentrations, together with RhB calibration curve. Dye concentrations of the solutions presented in this Figure are reported in Table S1 and in Table S3.

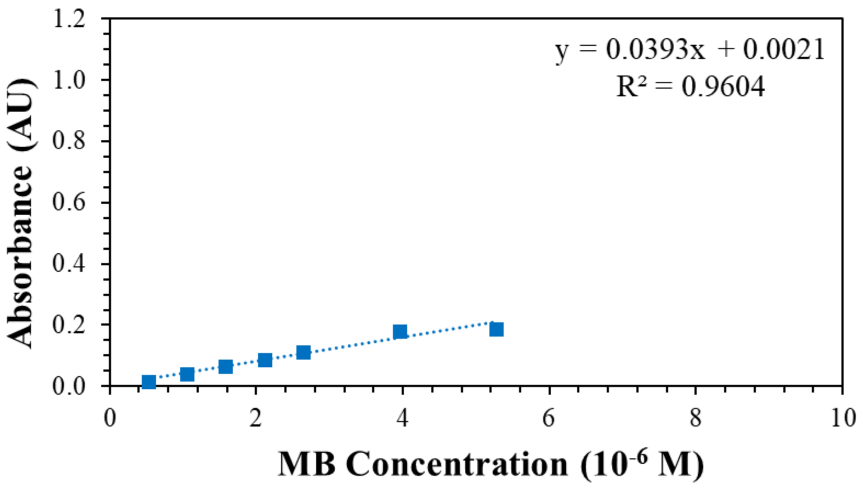

Figure S13. MB calibration curve in DR80 + MB + RhB system, evaluated at MB maximum absorbance peak (690 nm).

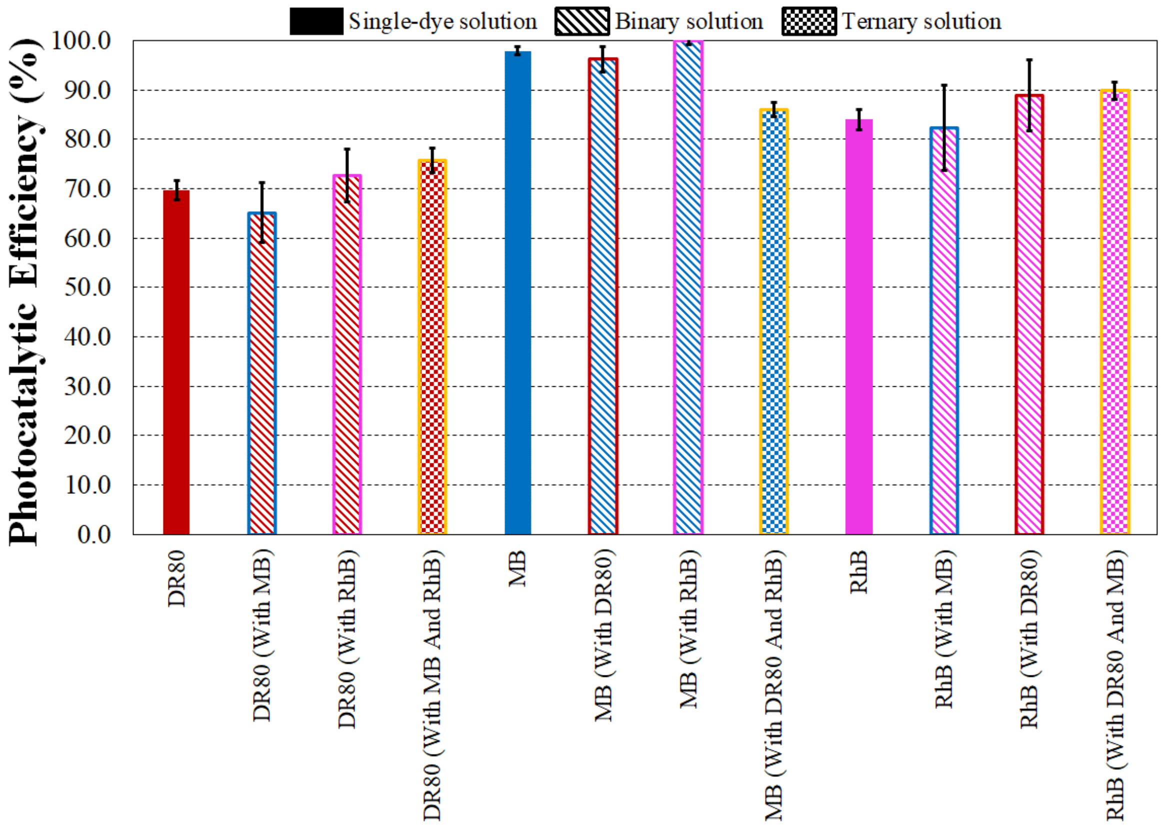

Figure S14. Photocatalytic efficiency for the evaluated conditions.

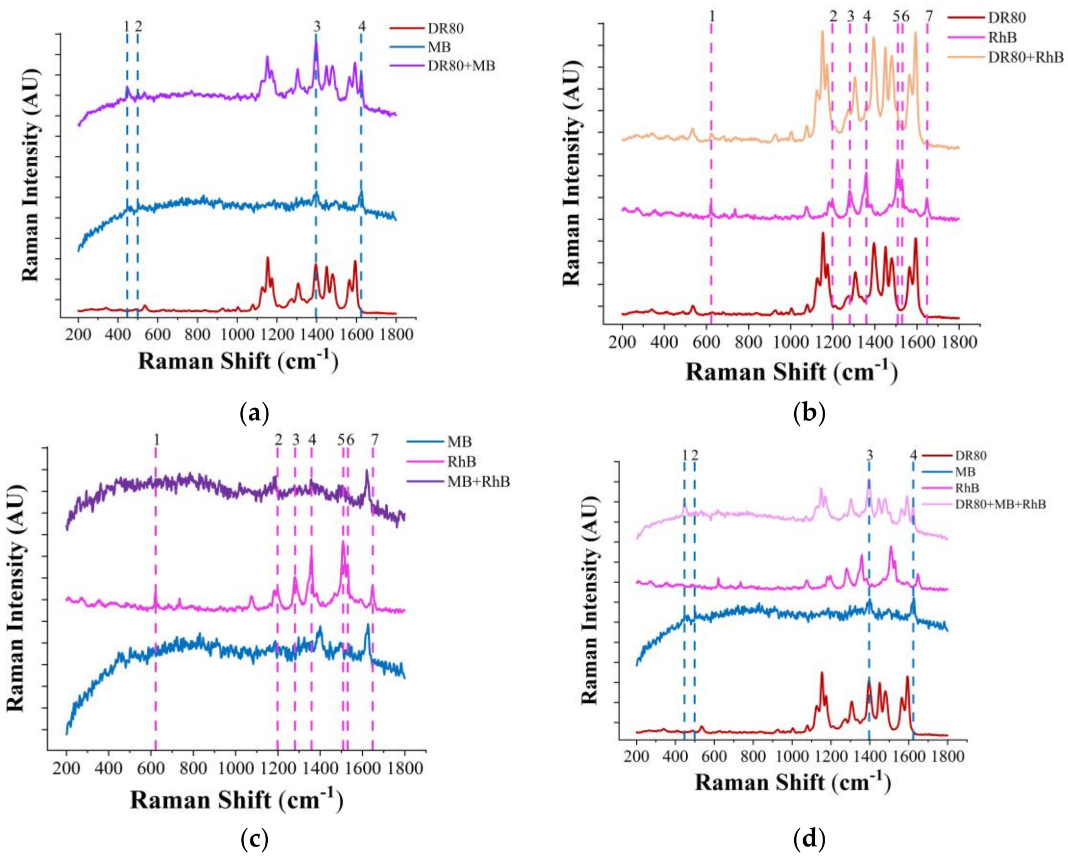

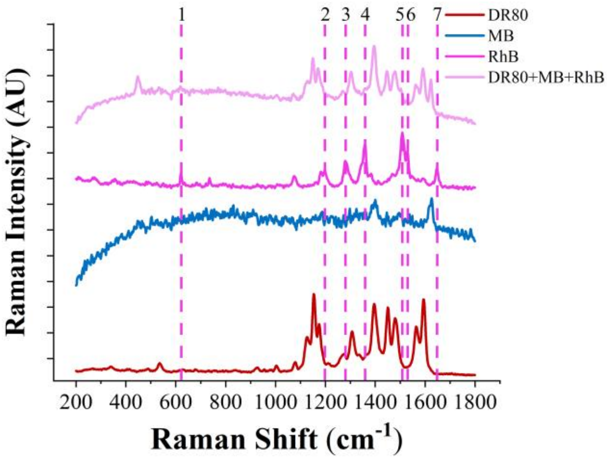

(**e**)

Figure S15. (**a**) Raman spectra of DR80, MB and DR80 + MB (dashed lines indicate peaks of MB). (**b**) Raman spectra of DR80, RhB and DR80 + RhB (dashed lines indicate peaks of RhB). (**c**) Raman spectra of MB, RhB and MB + RhB (dashed lines indicate peaks of RhB). (**d**) Raman spectra of DR80, MB, RhB and DR80 + MB + RhB (dashed lines indicate peaks of MB). (**e**) Raman spectra of DR80, MB, RhB and DR80 + MB + RhB (dashed lines indicate peaks of RhB).

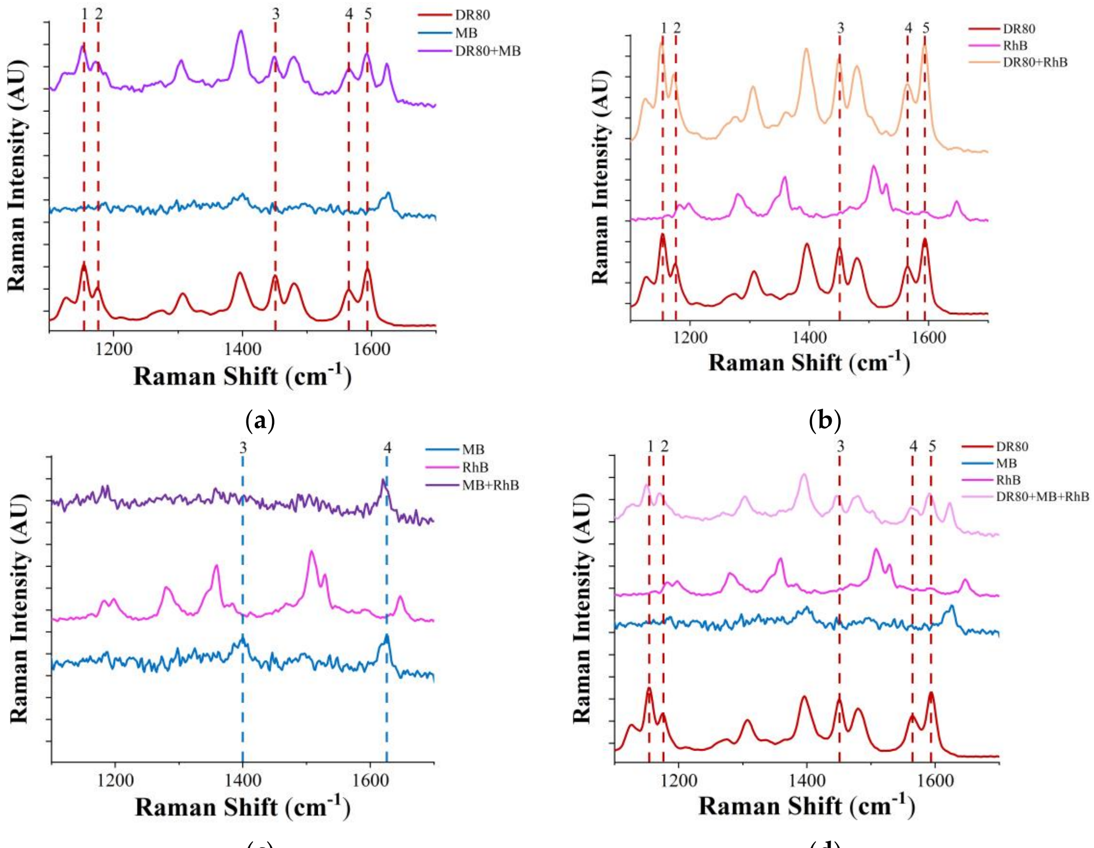

(**a**) (**b**)

(**c**) (**d**)

Figure S16. (**a**) Raman spectra of DR80, MB and DR80 + MB (peaks of DR80, zoom in the range 1100–1700 cm^{-1}). (**b**) Raman spectra of DR80, RhB and DR80 + RhB (peaks of DR80, zoom in the range 1100–1700 cm^{-1}). (**c**) Raman spectra of MB, RhB and MB + RhB (peaks of MB, zoom in the range 1100–1700 cm^{-1}). (**d**) Raman spectra of DR80, MB, RhB and DR80+MB+RhB (peaks of DR80, zoom in the range 1100–1700 cm^{-1}).

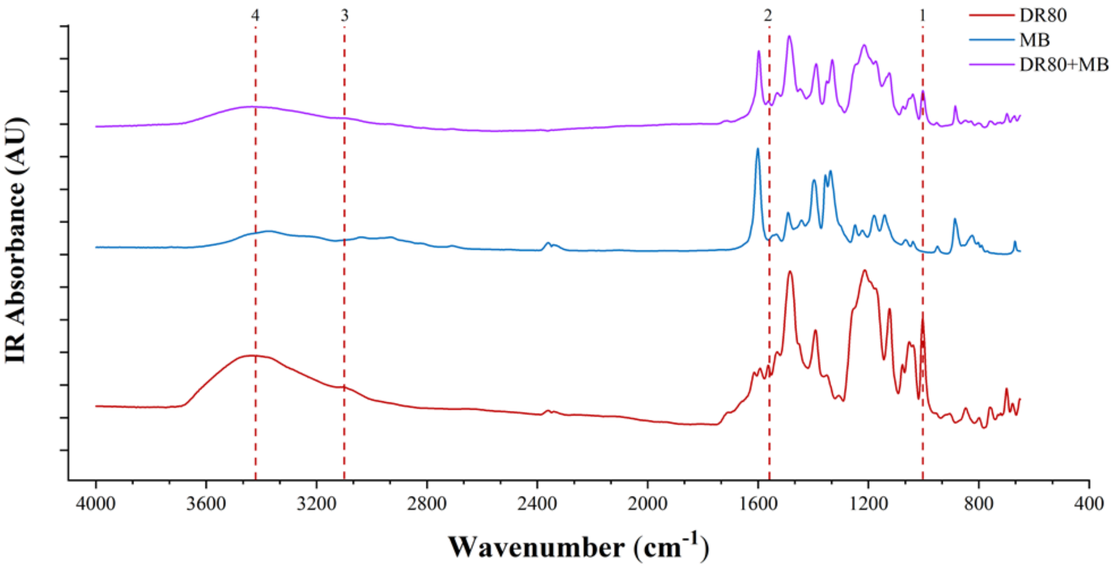

(**a**)

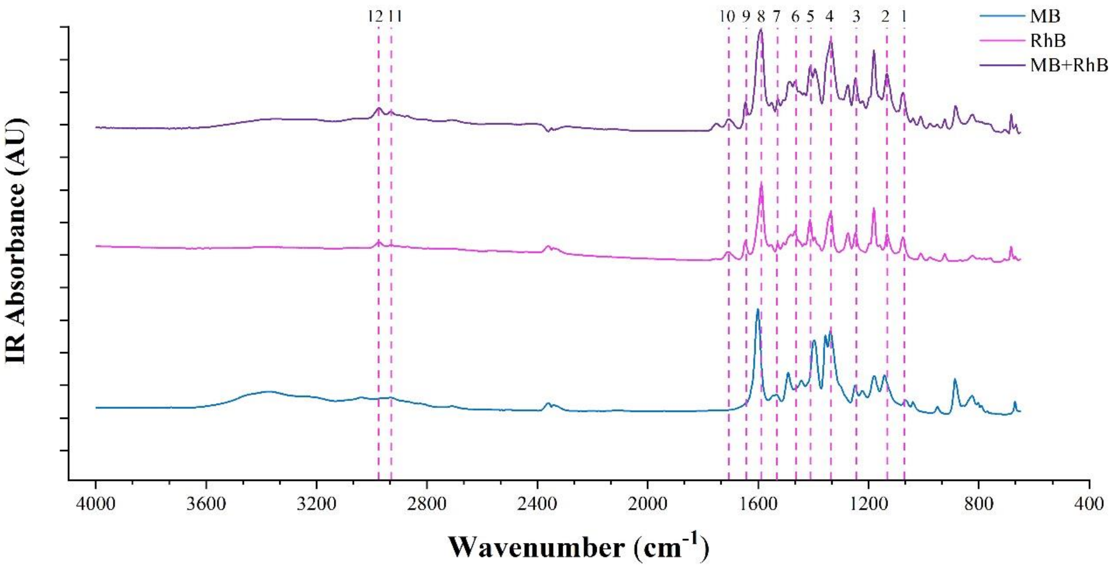

(**b**)

Figure S17. (**a**) FTIR spectra of DR80, MB and DR80 + MB (dashed lines indicate peaks of DR80). (**b**) FTIR spectra of MB, RhB and MB + RhB (dashed lines indicate peaks of RhB).

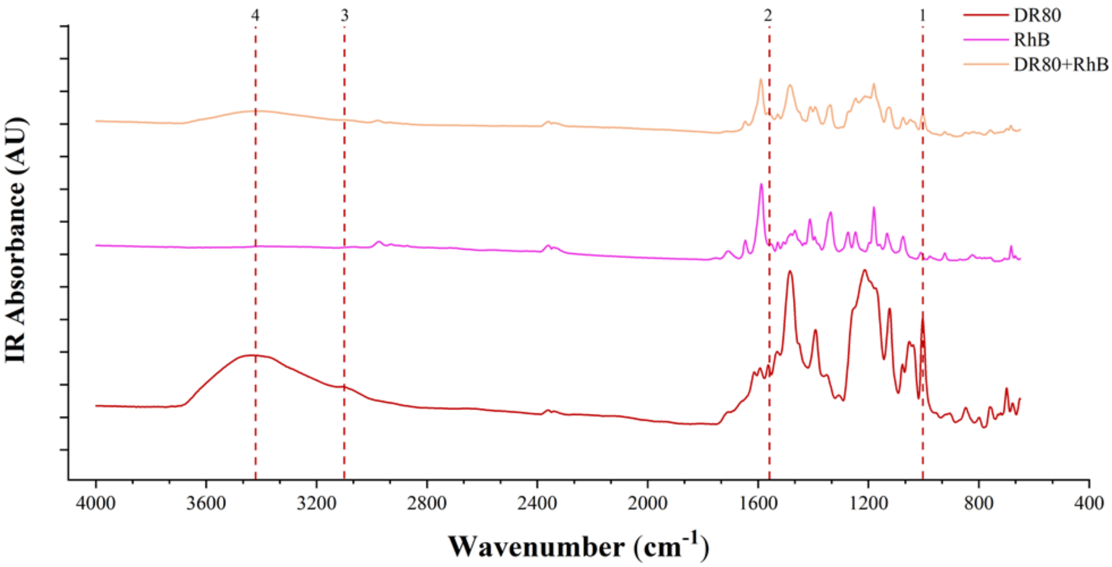

(**a**)

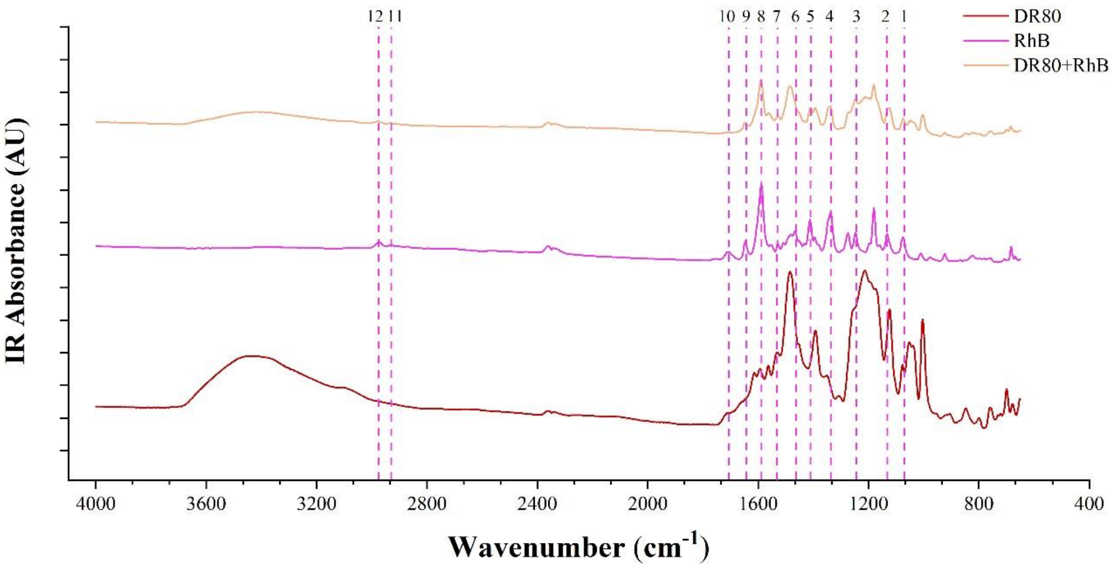

(**b**)

Figure S18. (**a**) FTIR spectra of DR80, RhB and DR80 + RhB (dashed lines indicate peaks of DR80). (**b**) FTIR spectra of DR80, RhB and DR80 + RhB (dashed lines indicate peaks of RhB).

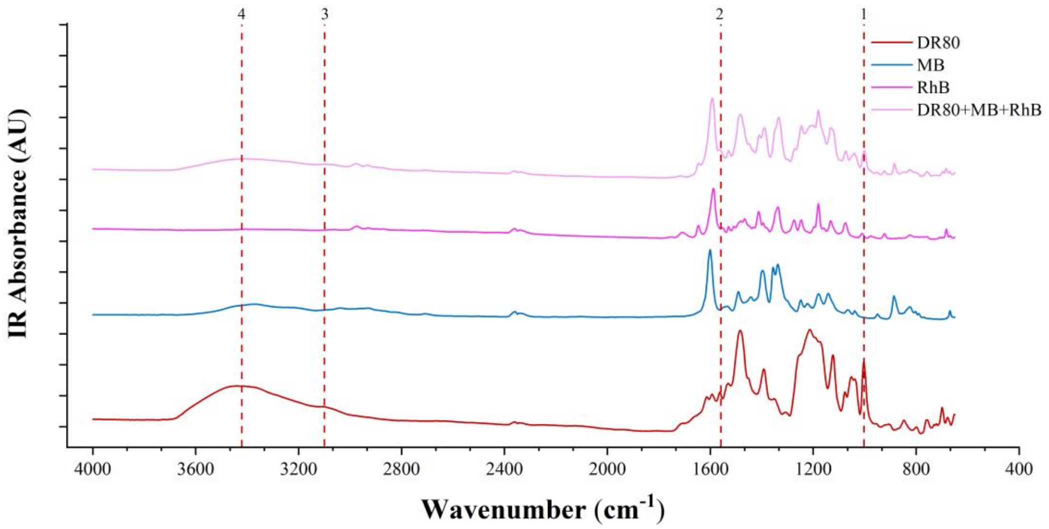

(**a**)

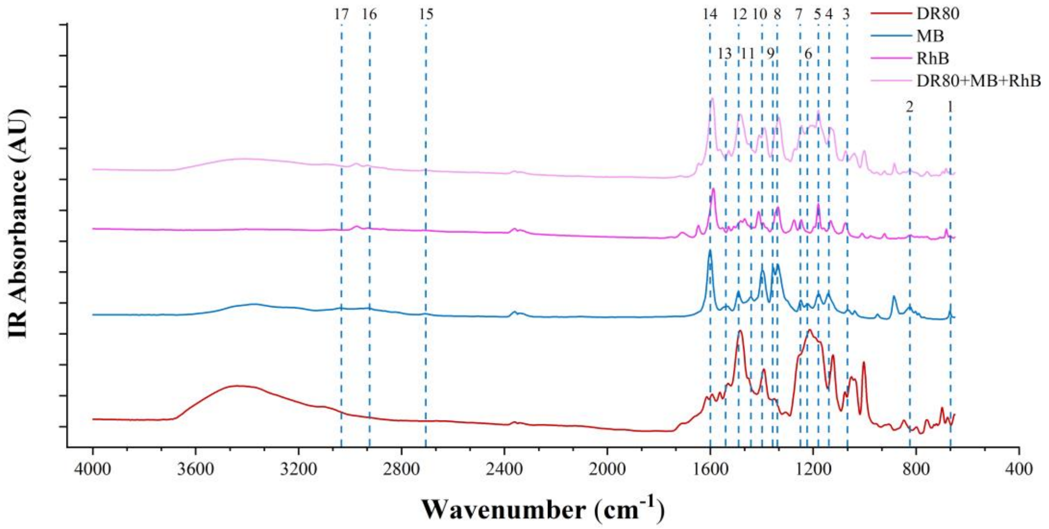

(**b**)

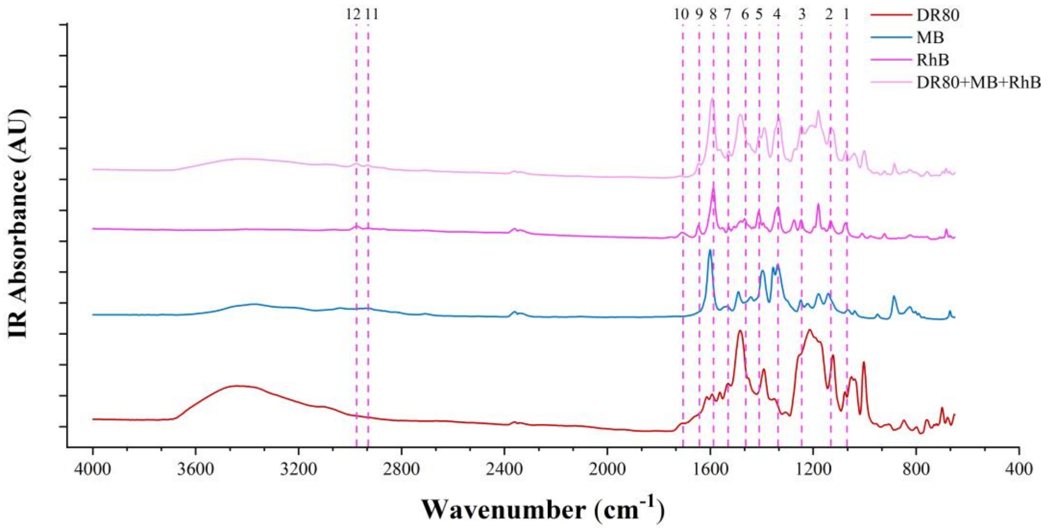

(**c**)

Figure S19. (**a**) FTIR spectra of DR80, MB, RhB and DR80 + MB + RhB (dashed lines indicate peaks of DR80). (**b**) FTIR spectra of DR80, MB, RhB and DR80 + MB + RhB (dashed lines indicate peaks of MB). (**c**) FTIR spectra of DR80, MB, RhB and DR80 + MB + RhB (dashed lines indicate peaks of RhB).

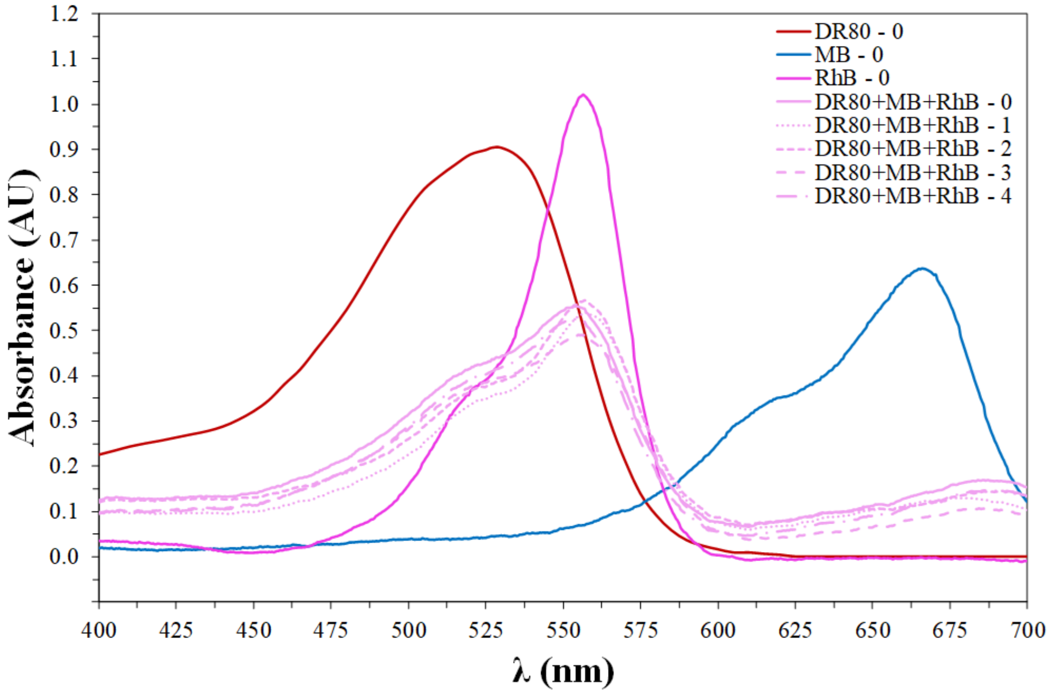

Figure S20. Absorbance spectra of DR80 + MB + RhB and single-dye solutions. 0 refers to pH 6 solution, without addition of salts; 1 refers to pH 6 solution with the addition of 2 M of NaCl; 2 refers to pH 6 solution with the addition of 1 M of Na_2SO_4; 3 refers to acidic solution (pH 2.5–3); 4 refers to basic solution (pH 11.5–12).

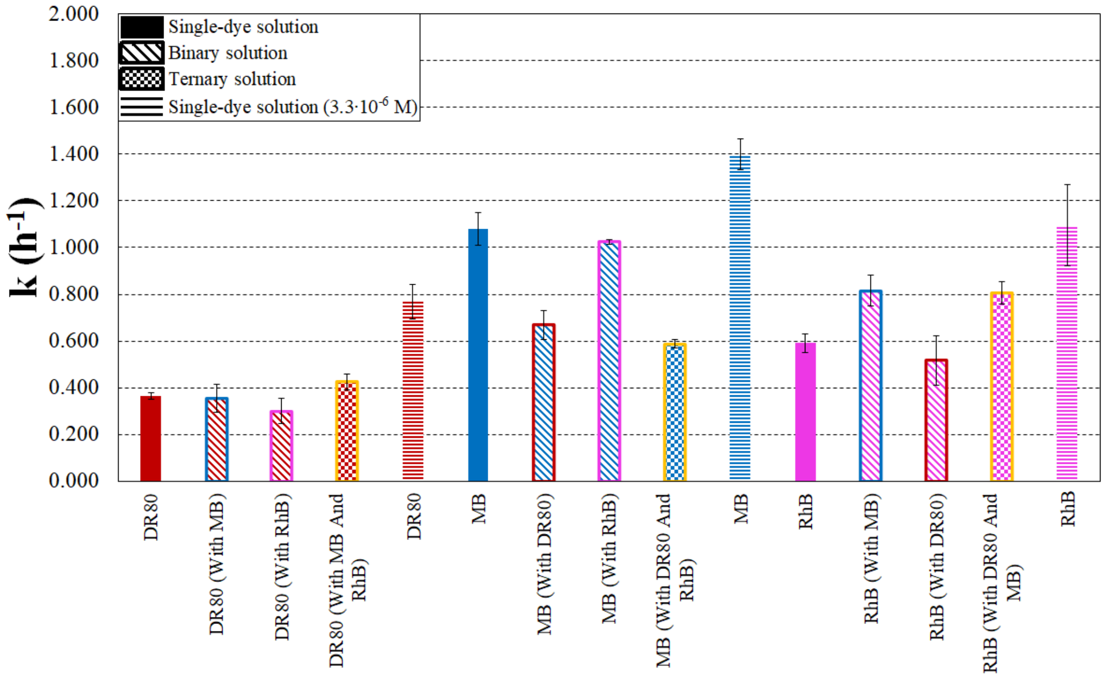

Figure S21. Photocatalytic kinetics of both the studied conditions and single-dye solutions with concentration 3.3×10^{-6} M.

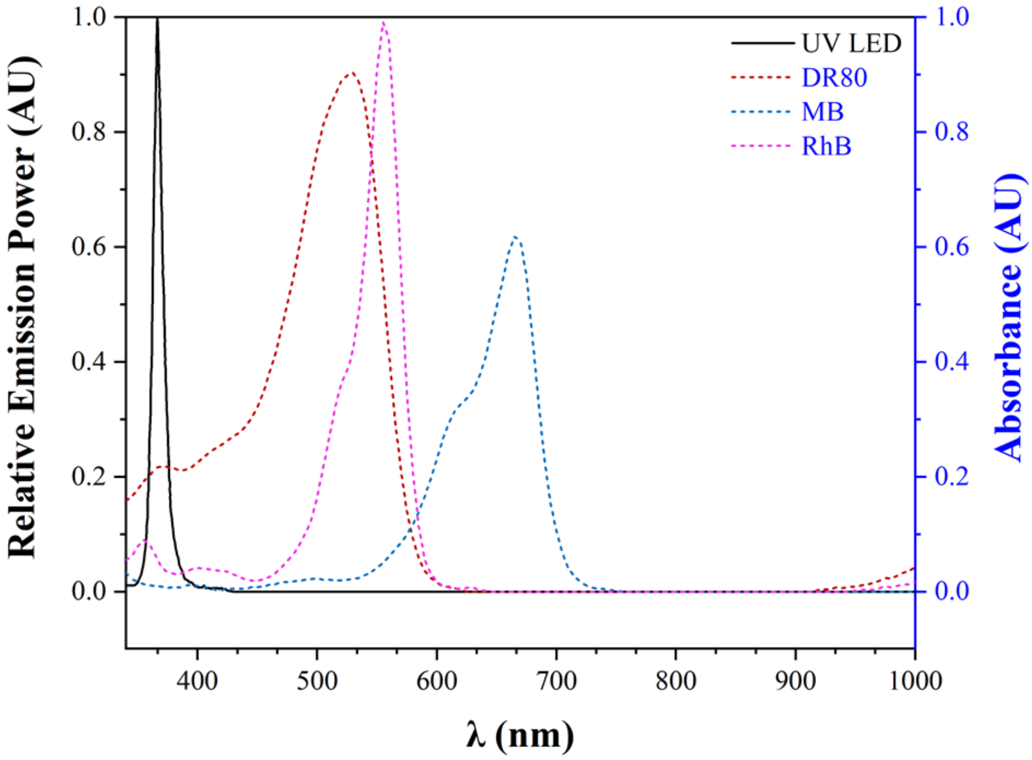

Figure S22. Relative emission power of the UV LED (black line); the dotted lines refers to the absorbance of DR80,MB and RhB in the range 350–1000 nm.

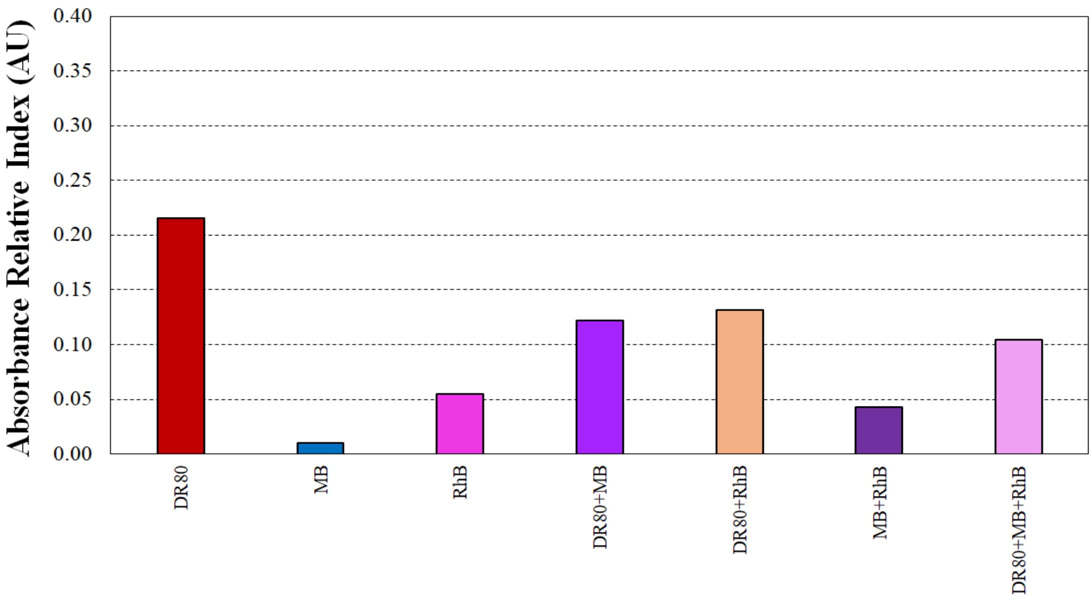

Figure S23. Absorbance relative index (ARI) for the evaluated conditions.

Table S1. Solutions used for DR80, MB and RhB calibration in single-dye solutions (italic) and for the analysis of coincident points in ternary solutions (the theoretical concentration C_t is expressed in 10^{-6} M).

Samples	DR80 C_t	Samples	MB C_t	Samples	RhB C_t
DR80 - 1	5.65	*MB - 1*	7.90	*RhB - 1*	5.00
DR80 - 2	1.88	*MB - 2*	2.63	*RhB - 2*	1.67
DR80 - 3	11.30	*MB - 3*	15.80	*RhB - 3*	10.00
DR80 - 4	3.77	*MB - 4*	5.27	*RhB - 4*	3.33
DR80 - 5	1.13	*MB - 5*	1.58	*RhB - 5*	1.00
DR80 - 6	2.26	MB - 6	3.16	RhB - 6	2.00
DR80 - 7	0.75	MB - 7	1.05	RhB - 7	0.67
DR80 - 8	3.39	MB - 8	4.74	RhB - 8	3.00
DR80 - 9	4.52	MB - 9	6.32	RhB - 9	4.00
DR80 - 10	8.48	MB - 10	11.85	RhB - 10	7.50
DR80 - 11	0.38	MB - 11	0.53	RhB - 11	0.33
DR80 - 12	1.13	MB - 12	1.58	RhB - 12	1.00
DR80 - 13	1.51	MB - 13	2.11	RhB - 13	1.33
DR80 - 14	2.83	MB - 14	3.95	RhB - 14	2.50
DR80 - 15	0.71	MB - 15	0.99	RhB - 15	0.63
DR80 - 16	1.41	MB - 16	1.98	RhB - 16	1.25

Table S2. Binary solutions used for DR80, MB and RhB calibration in binary mixtures (the theoretical concentration C_t is expressed in 10^{-6} M).

Samples	DR80 + MB		Samples	DR80 + RhB		Samples	MB + RhB	
	C_t (DR80)	C_t (MB)		C_t (DR80)	C_t (RhB)		C_t (MB)	C_t (RhB)
DR80+MB - 1	2.83	3.95	DR80+RhB - 1	2.83	2.50	MB+RhB - 1	3.95	2.50
DR80+MB - 2	0.00	3.95	DR80+RhB - 2	0.00	2.50	MB+RhB - 2	0.00	2.50
DR80+MB - 3	0.57	3.95	DR80+RhB - 3	0.57	2.50	MB+RhB - 3	0.79	2.50
DR80+MB - 4	1.13	3.95	DR80+RhB - 4	1.13	2.50	MB+RhB - 4	1.58	2.50
DR80+MB - 5	1.70	3.95	DR80+RhB - 5	1.70	2.50	MB+RhB - 5	2.37	2.50
DR80+MB - 6	2.26	3.95	DR80+RhB - 6	2.26	2.50	MB+RhB - 6	3.16	2.50
DR80+MB - 7	4.24	3.95	DR80+RhB - 7	4.24	2.50	MB+RhB - 7	5.93	2.50
DR80+MB - 8	5.65	3.95	DR80+RhB - 8	5.65	2.50	MB+RhB - 8	7.90	2.50
DR80+MB - 9	2.83	0.00	DR80+RhB - 9	2.83	0.00	MB+RhB - 9	3.95	0.00
DR80+MB - 10	2.83	0.79	DR80+RhB - 10	2.83	0.50	MB+RhB - 10	3.95	0.50
DR80+MB - 11	2.83	1.58	DR80+RhB - 11	2.83	1.00	MB+RhB - 11	3.95	1.00
DR80+MB - 12	2.83	2.37	DR80+RhB - 12	2.83	1.50	MB+RhB - 12	3.95	1.50
DR80+MB - 13	2.83	3.16	DR80+RhB - 13	2.83	2.00	MB+RhB - 13	3.95	2.00
DR80+MB - 14	2.83	5.93	DR80+RhB - 14	2.83	3.75	MB+RhB - 14	3.95	3.75
DR80+MB - 15	2.83	7.90	DR80+RhB - 15	2.83	5.00	MB+RhB - 15	3.95	5.00

Table S3. Ternary solutions used for DR80, MB and RhB calibration in DR80 + MB + RhB solution (the theoretical concentration C_t is expressed in 10^{-6} M).

Samples	**DR80 + MB + RhB**		
	C_t (DR80)	**C_t (MB)**	**C_t (RhB)**
DR80 + MB + RhB - 1	1.88	2.63	1.67
DR80 + MB + RhB - 2	0.00	2.63	1.67
DR80 + MB + RhB - 3	0.38	2.63	1.67
DR80 + MB + RhB - 4	0.75	2.63	1.67
DR80 + MB + RhB - 5	1.13	2.63	1.67
DR80 + MB + RhB - 6	1.51	2.63	1.67
DR80 + MB + RhB - 7	2.83	2.63	1.67
DR80 + MB + RhB - 8	3.77	2.63	1.67
DR80 + MB + RhB - 9	1.88	0.00	1.67
DR80 + MB + RhB - 10	1.88	0.53	1.67
DR80 + MB + RhB - 11	1.88	1.05	1.67
DR80 + MB + RhB - 12	1.88	1.58	1.67
DR80 + MB + RhB - 13	1.88	2.11	1.67
DR80 + MB + RhB - 14	1.88	3.95	1.67
DR80 + MB + RhB - 15	1.88	5.27	1.67
DR80 + MB + RhB - 16	1.88	2.63	0.00
DR80 + MB + RhB - 17	1.88	2.63	0.33
DR80 + MB + RhB - 18	1.88	2.63	0.67
DR80 + MB + RhB - 19	1.88	2.63	1.00
DR80 + MB + RhB - 20	1.88	2.63	1.33
DR80 + MB + RhB - 21	1.88	2.63	2.50
DR80 + MB + RhB - 22	1.88	2.63	3.33
DR80 + MB + RhB - 23	5.65	7.90	5.00

Table S4. Regression analysis for the calibration curves in single-dye, binary and ternary mixtures (S.E. = Standard error, RSE = Standard error of the estimate).

Method	Analyte	Solution	Wavelength (nm)	Regression Equation	S.E. of Slope	S.E. of Intercept	R^2	RSE	LOD (10^{-6} M)
Beer-Lambert law	DR80	DR80	527	$y = 0.0894x^a + 0.0011$	0.00101	0.00591	0.9996	0.00873	0.29
-	MB	MB	666	$y = 0.0628x^a + 0.0084$	0.00054	0.00444	0.9998	0.00656	0.31
-	RhB	RhB	555	$y = 0.1031x^a - 0.0003$	0.00085	0.00437	0.9998	0.00646	0.19
-	MB	DR80+MB	690	$y = 0.0369x^a + 0.0212$	0.00301	0.01307	0.9677	0.01849	1.50
-	MB	DR80+MB+RhB	690	$y = 0.0393x^a + 0.0021$	0.00356	0.01031	0.9604	0.01458	1.11
-	-	-	-	-	-	-	-	-	-
Zero-crossing first order derivative spectrophotometry	DR80	DR80+MB	505	$y = 0.000708x^b - 0.000162$	0.0000583	0.0001810	0.9672	0.0002560	1.08
	MB	DR80+MB	675	$y = 0.000232x^b + 0.000815$	0.0000504	0.0002185	0.8095	0.0003090	3.99
-	-	-	-	-	-	-	-	-	-
-	DR80	DR80+RhB	555	$y = -0.002031x^b - 0.000662$	0.0001435	0.0004454	0.9757	0.0006299	0.93
-	RhB	DR80+RhB	525	$y = 0.000612x^b + 0.000208$	0.0000632	0.0001736	0.9494	0.0002455	1.20
-	-	-	-	-	-	-	-	-	-
-	MB	MB+RhB	685	$y = -0.001993x^b - 0.000272$	0.0000559	0.0002426	0.9961	0.0003431	0.52
-	RhB	MB+RhB	505	$y = 0.001103x^b - 0.000285$	0.0000444	0.0001220	0.9920	0.0001725	0.47
-	-	-	-	-	-	-	-	-	-
Double divisor ratio spectra derivative spectrophotometry	DR80	DR80+MB+RhB	500	$y = -0.0847x^c - 0.0010$	0.00151	0.00313	0.9984	0.00443	0.16
	RhB	DR80+MB+RhB	550	$y = 0.0189x^c - 0.0015$	0.00042	0.00077	0.9975	0.00109	0.17

a: x^a is molar concentration in 10^{-6} M, y is absorbance.

b: x^b is molar concentration in 10^{-6} M, y is $dA/d\lambda$.

c: x^c is molar concentration in 10^{-6} M, y is $d/d\lambda$ [$A_{TERNARY}/A_{MB+RhB}$] or $d/d\lambda$ [$A_{TERNARY}/A_{DR80+MB}$].

d: x^d is molar concentration in 10^{-6} M, y is $d/d\lambda$ [A_{DR80}/A_{MB+RhB}] or $d/d\lambda$ [$A_{RhB}/A_{DR80+MB}$].

Table S5. Analysis of accuracy for DR80 in single-dye solution (the theoretical concentration C_t and the measured concentration C_m are expressed in 10^{-6} M).

Samples	DR80 C_t	λ = 527 nm C_m	λ = 527 nm Recovery (%)	λ = 527 nm Error (%)
DR80 - 15	0.71	0.77	109.19	9.19
DR80 - 16	1.41	1.27	90.24	9.76
DR80 - 14	2.83	2.90	102.56	2.56
DR80 - 1	5.65	5.66	100.20	0.20
DR80 - 3	11.30	11.29	99.91	0.09
-	-	$\bar{x}$ = 100.42 ± 3.04, S.D. = 6.81, RSD = 6.78%		

Table S6. Analysis of accuracy for MB in single-dye solution (the theoretical concentration C_t and the measured concentration C_m are expressed in 10^{-6} M).

Samples	MB C_t	λ = 666 nm C_m	λ = 666 nm Recovery (%)	λ = 666 nm Error (%)
MB - 15	0.99	1.00	100.89	0.89
MB - 16	1.98	1.86	93.97	6.03
MB - 14	3.95	4.08	103.41	3.41
MB - 1	7.90	7.89	99.87	0.13
MB - 3	15.80	15.79	99.91	0.09
-	-	$\bar{x}$ = 99.61 ± 1.55, S.D. = 3.46, RSD = 3.48%		

Table S7. Analysis of accuracy for RhB in single-dye solution (the theoretical concentration C_t and the measured concentration C_m are expressed in 10^{-6} M).

Samples	RhB C_t	λ = 555 nm C_m	λ = 555 nm Recovery (%)	λ = 555 nm Error (%)
RhB - 15	0.63	0.65	104.43	4.43
RhB - 16	1.25	1.17	93.34	6.66
RhB - 14	2.50	2.56	102.54	2.54
RhB - 1	5.00	5.00	99.96	0.04
RhB - 3	10.00	9.99	99.94	0.06
-	-	$\bar{x}$ = 100.04 ± 1.88, S.D. = 4.20, RSD = 4.19%		

Table S8. Analysis of accuracy for DR80 + MB (the theoretical concentration C_t and the measured concentration C_m are expressed in 10^{-6} M).

Samples	DR80 + MB		DR80, λ = 505 nm			MB, λ = 675 nm			MB, λ = 690 nm		
	C_t (DR80)	C_t (MB)	C_m	Recovery (%)	Error (%)	C_m	Recovery (%)	Error (%)	C_m	Recovery (%)	Error (%)
DR80+MB - 3	0.57	3.95	0.51	90.40	9.60	-17.05	-431.76	531.76	1.16	29.39	70.61
DR80+MB - 4	1.13	3.95	0.79	70.21	29.79	-5.98	-151.27	251.27	1.38	34.89	65.11
DR80+MB - 5	1.70	3.95	1.64	96.81	3.19	0.80	20.14	79.86	3.55	89.82	10.18
DR80+MB - 6	2.26	3.95	2.49	110.12	10.12	4.49	113.63	13.63	4.04	102.18	2.18
DR80+MB - 1	2.83	3.95	3.43	121.43	21.43	5.39	136.49	36.49	4.88	123.46	23.46
DR80+MB - 7	4.24	3.95	3.90	92.07	7.93	7.69	194.66	94.66	5.09	128.95	28.95
DR80+MB - 8	5.65	3.95	5.60	99.06	0.94	6.83	172.85	72.85	4.93	124.83	24.83
-	-	-	$\bar{x}$ = 97.16 ± 6.09, S.D. = 16.12, RSD = 16.59%			$\bar{x}$ = 7.82 ± 85.72, S.D. = 226.79, RSD = 2900.11%			$\bar{x}$ = 90.50 ± 15.97, S.D. = 42.24, RSD = 46.68%		
DR80+MB - 10	2.83	0.79	2.91	103.10	3.10	-0.07	-8.39	108.39	0.46	57.70	42.30
DR80+MB - 11	2.83	1.58	2.63	93.10	6.90	-0.07	-4.20	104.20	1.30	82.07	17.93
DR80+MB - 12	2.83	2.37	2.77	98.10	1.90	3.38	142.64	42.64	2.41	101.63	1.63
DR80+MB - 13	2.83	3.16	2.63	93.10	6.90	4.24	134.25	34.25	3.20	101.11	1.11
DR80+MB - 1	2.83	3.95	3.43	121.43	21.43	5.39	136.49	36.49	4.88	123.46	23.46
DR80+MB - 14	2.83	5.93	2.49	88.09	11.91	5.97	100.69	0.69	5.99	101.08	1.08
DR80+MB - 15	2.83	7.90	2.77	98.10	1.90	6.83	86.42	13.58	7.45	94.35	5.65
-	-	-	$\bar{x}$ = 99.29 ± 4.11, S.D. = 10.88, RSD = 10.95%			$\bar{x}$ = 83.99 ± 24.55, S.D. = 64.96, RSD = 77.34%			$\bar{x}$ = 94.48 ± 7.69, S.D. = 20.35, RSD = 21.54%		

Table S9. Analysis of accuracy for DR80 + RhB (the theoretical concentration C_t and the measured concentration C_m are expressed in 10^{-6} M).

Samples	DR80 + RhB		DR80, λ = 505 nm			RhB, λ = 525 nm		
	C_t (DR80)	C_t (RhB)	C_m	Recovery (%)	Error (%)	C_m	Recovery (%)	Error (%)
DR80+RhB - 3	0.57	2.50	0.66	116.61	16.61	2.27	90.99	9.01
DR80+RhB - 4	1.13	2.50	1.25	110.58	10.58	2.60	104.06	4.06
DR80+RhB - 5	1.70	2.50	1.45	85.34	14.66	2.44	97.53	2.47
DR80+RhB - 6	2.26	2.50	1.84	81.43	18.57	2.76	110.60	10.60
DR80+RhB - 1	2.83	2.50	3.28	116.26	16.26	3.26	130.20	30.20
DR80+RhB - 7	4.24	2.50	4.30	101.51	1.51	2.93	117.13	17.13
DR80+RhB - 8	5.65	2.50	5.58	98.79	1.21	2.60	104.06	4.06
-	-	-	$\bar{x}$ = 101.50 ± 5.35, S.D. = 14.14, RSD = 13.93%			$\bar{x}$ = 107.79 ± 4.91, S.D. = 12.99, RSD = 12.05%		
DR80+RhB - 10	2.83	0.50	2.82	99.99	0.01	0.31	62.84	37.16
DR80+RhB - 11	2.83	1.00	2.82	99.99	0.01	0.97	96.77	3.23
DR80+RhB - 12	2.83	1.50	2.82	99.99	0.01	1.62	108.08	8.08
DR80+RhB - 13	2.83	2.00	2.63	93.02	6.98	1.62	81.06	18.94
DR80+RhB - 1	2.83	2.50	3.28	116.26	16.26	3.26	130.20	30.20
DR80+RhB - 14	2.83	3.75	3.02	106.96	6.96	3.58	95.51	4.49
DR80+RhB - 15	2.83	5.00	3.12	110.45	10.45	4.89	97.78	2.22
-	-	-	$\bar{x}$ = 103.81 ± 2.96, S.D. = 7.84, RSD = 7.55%			$\bar{x}$ = 96.03 ± 7.93, S.D. = 20.99, RSD = 21.85%		

Table S10. Analysis of accuracy for MB + RhB (the theoretical concentration C_t and the measured concentration C_m are expressed in 10^{-6} M).

Samples	MB + RhB		MB, λ = 685 nm			RhB, λ = 525 nm		
	C_t (DR80)	C_t (RhB)	C_m	Recovery (%)	Error (%)	C_m	Recovery (%)	Error (%)
MB+RhB - 3	0.79	2.50	0.87	109.78	9.78	2.61	104.60	4.60
MB+RhB - 4	1.58	2.50	1.54	97.24	2.76	2.19	87.68	12.32
MB+RhB - 5	2.37	2.50	2.34	98.70	1.30	2.19	87.68	12.32
MB+RhB - 6	3.16	2.50	2.91	92.02	7.98	2.49	99.76	0.24
MB+RhB - 1	3.95	2.50	4.15	104.96	4.96	2.55	102.18	2.18
MB+RhB - 7	5.93	2.50	6.09	102.72	2.72	3.16	126.36	26.36
MB+RhB - 8	7.90	2.50	7.79	98.64	1.36	2.80	111.85	11.85
-	-	-	$\bar{x}$ = 100.58 ± 2.18, S.D. = 5.77, RSD = 5.74%			$\bar{x}$ = 102.87 ± 5.13, S.D. = 13.58, RSD = 13.20%		
MB+RhB - 10	3.95	0.50	4.08	103.26	3.26	0.62	124.12	24.12
MB+RhB - 11	3.95	1.00	3.88	98.18	1.82	0.98	98.32	1.68
MB+RhB - 12	3.95	1.50	3.88	98.18	1.82	1.53	101.81	1.81
MB+RhB - 13	3.95	2.00	3.98	100.72	0.72	1.71	85.42	14.58
MB+RhB - 1	3.95	2.50	4.15	104.96	4.96	2.55	102.18	2.18
MB+RhB - 14	3.95	3.75	3.98	100.72	0.72	3.88	103.58	3.58
MB+RhB - 15	3.95	5.00	3.78	95.64	4.36	4.97	99.44	0.56
-	-	-	$\bar{x}$ = 100.23 ± 1.21, S.D. = 3.20, RSD = 3.19%			$\bar{x}$ = 102.12 ± 4.33, S.D. = 11.45, RSD = 11.21%		

Table S11. Analysis of accuracy for DR80 + MB + RhB (the theoretical concentration C_t and the measured concentration C_m are expressed in 10^{-6} M).

Samples	DR80 + MB + RhB			DR80, λ = 500 nm			MB, λ = 690 nm			RhB, λ = 550 nm		
	C_t (DR80)	C_t (MB)	C_t (RhB)	C_m	Recovery (%)	Error (%)	C_m	Recovery (%)	Error (%)	C_m	Recovery (%)	Error (%)
DR80+MB+RhB - 3	0.38	2.63	1.67	0.45	120.20	20.20	1.60	60.81	39.19	2.04	122.38	22.38
DR80+MB+RhB - 4	0.75	2.63	1.67	0.67	88.79	11.21	2.19	83.05	16.95	2.02	121.42	21.42
DR80+MB+RhB - 5	1.13	2.63	1.67	1.14	101.28	1.28	2.59	98.52	1.48	1.95	116.94	16.94
DR80+MB+RhB - 6	1.51	2.63	1.67	1.50	99.53	0.47	2.67	101.42	1.42	1.78	107.02	7.02
DR80+MB+RhB - 1 (DR80)	1.88	2.63	1.67	1.87	99.05	0.95	2.82	107.22	7.22	1.69	101.59	1.59
DR80+MB+RhB - 7	2.83	2.63	1.67	2.83	100.30	0.30	3.05	115.93	15.93	1.59	95.51	4.49
DR80+MB+RhB - 8	3.77	2.63	1.67	3.78	100.27	0.27	3.21	121.73	21.73	1.57	94.07	5.93
-	-	-	-	$\bar{x}$ = 101.25 ± 3.53, S.D. = 9.34, RSD = 9.22%			$\bar{x}$ = 98.38 ± 7.85, S.D. = 20.76, RSD = 21.11%			$\bar{x}$ = 108.42 ± 4.52, S.D. = 11.96, RSD = 11.03%		
DR80+MB+RhB - 10	1.88	0.53	1.67	1.90	100.86	0.86	0.30	57.46	42.54	1.12	67.36	32.64
DR80+MB+RhB - 11	1.88	1.05	1.67	1.88	99.95	0.05	0.96	91.58	8.42	1.44	86.55	13.45
DR80+MB+RhB - 12	1.88	1.58	1.67	1.90	100.86	0.86	1.60	101.35	1.35	1.46	87.51	12.49
DR80+MB+RhB - 13	1.88	2.11	1.67	1.93	102.74	2.74	2.14	101.39	1.39	1.61	96.47	3.53
DR80+MB+RhB - 1 (MB)	1.88	2.63	1.67	1.87	99.05	0.95	2.82	107.22	7.22	1.69	101.59	1.59
DR80+MB+RhB - 14	1.88	3.95	1.67	1.92	101.92	1.92	4.53	114.67	14.67	1.80	107.79	7.79
DR80+MB+RhB - 15	1.88	5.27	1.67	2.11	112.09	12.09	4.76	90.36	9.64	1.79	107.15	7.15
-	-	-	-	$\bar{x}$ = 102.50 ± 1.66, S.D. = 4.40, RSD = 4.29%			$\bar{x}$ = 94.86 ± 7.00, S.D. = 18.53, RSD = 19.53%			$\bar{x}$ = 93.49 ± 5.42, S.D. = 14.33, RSD = 15.33%		
DR80+MB+RhB - 17	1.88	2.63	0.33	1.96	104.30	4.30	3.03	114.96	14.96	0.29	87.24	12.76
DR80+MB+RhB - 18	1.88	2.63	0.67	1.98	105.12	5.12	2.95	112.06	12.06	0.61	91.61	8.39
DR80+MB+RhB - 19	1.88	2.63	1.00	1.94	103.07	3.07	3.00	113.99	13.99	1.04	104.26	4.26
DR80+MB+RhB - 20	1.88	2.63	1.33	1.89	100.28	0.28	2.82	107.22	7.22	1.38	103.39	3.39
DR80+MB+RhB - 1 (RhB)	1.88	2.63	1.67	1.87	99.05	0.95	2.82	107.22	7.22	1.69	101.59	1.59
DR80+MB+RhB - 21	1.88	2.63	2.50	1.88	99.79	0.21	3.00	113.99	13.99	2.55	102.06	2.06
DR80+MB+RhB - 22	1.88	2.63	3.33	2.00	106.02	6.02	2.90	110.12	10.12	3.27	97.98	2.02
-	-	-	-	$\bar{x}$ = 102.52 ± 1.06, S.D. = 2.80, RSD = 2.73%			$\bar{x}$ = 111.37 ± 1.22, S.D. = 3.24, RSD = 2.91%			$\bar{x}$ = 98.30 ± 2.46, S.D. = 6.50, RSD = 6.61%		

Table S12. Raman band assignments of selected marker bands of DR80, MB and RhB (Raman shift is expressed in cm^{-1}).

Peak		**DR80**	**Peak**		**MB**	**Peak**		**RhB**
-	**Raman Shift**	**Band Assignments and Modes**	**-**	**Raman Shift**	**Band Assignments and Modes**	**-**	**Raman Shift**	**Band Assignments and Modes**
1	1154	SO_3^- stretching	1	447	C–N–C skeletal deformation	1	622	Xantene ring puckering
2	1174	SO_3^- stretching	2	504	C–N–C skeletal deformation	2	1197	C–C bridge stretching
3	1448	N=N stretching	3	1398	C–H in plane ring deformation	3	1281	C–H bending
4	1565	C=N stretching	4	1624	C–C ring stretching	4	1359	Aromatic C–C bending
5	1594	C=C phenyl stretching	-	-	-	5	1507	Aromatic C–H bending
-	-	-	-	-	-	6	1529	Aromatic C–H bending
-	-	-	-	-	-	7	1646	C=C stretching, aromatic C–C bending

Table S13. The characteristic frequencies of FTIR bands of DR80, MB and RhB (FTIR band is expressed in cm^{-1}).

Peak		**DR80**	**Peak**		**MB**	**Peak**		**RhB**
-	**FTIR Band**	**Band Assignments and Modes**	**-**	**FTIR Band**	**Band Assignments and Modes**	**-**	**FTIR Band**	**Band Assignments and Modes**
1	1003	CO stretching	1	670	C–S–C stretching, C–N stretching	1	1075	CO stretching (C–O–H)
2	1565	C=N stretching	2	823	C–C in-plane bending	2	1132	C–O–C stretching
3	3100	C–H stretching	3	1066	C–S–C stretching	3	1248	C–N stretching $(=N^+(C_2H_6))$
4	3420	OH stretching	4	1142	C–N bending	4	1336	Aromatic ring–COOH C–C stretching and/or C–H bending
-	-	-	5	1180	C–H bending	5	1411	C–H bending $(=N^+(C_2H_6))$
-	-	-	6	1225	C–C stretching	6	1468	Aromatic ring vibrations
-	-	-	7	1248	C–H bending (in plane and out of plane)	7	1528	Aromatic ring vibrations
-	-	-	8	1338	C–N stretching	8	1590	Aromatic ring vibrations
-	-	-	9	1356	C=S stretching	9	1646	C=N stretching and/or C=C stretching

-	-	-	10	1397	C–H in-plane bending	10	1706	C=O stretching (COOH)
-	-	-	11	1444	C–H in-plane bending	11	2928	C–H stretching (CH_3)
-	-	-	12	1492	C=S stretching	12	2974	C–H stretching (CH_3)
-	-	-	13	1540	C–N stretching	-	-	-
-	-	-	14	1600	C=N stretching, C=C stretching	-	-	-
-	-	-	15	2709	C–H stretching (N–$(CH_3)_2$)	-	-	-
-	-	-	16	2926	C–H stretching (CH_3)	-	-	-
-	-	-	17	3380	OH stretching	-	-	-